Luminescent characteristics of $Tm^{3+}/Tb^{3+}/Eu^{3+}$ tri-doped $Na_5Y_9F_{32}$ single crystals for white emission with high thermal stability

Lizhi Fang(方立志)[1], Xiong Zhou(周雄)[1], Zhiwei Zhao(赵志伟)[2], Biao Zheng(郑标)[3], Haiping Xia(夏海平)[1,†], Jun Wang(王军)[3,‡], Hongwei Song(宋宏伟)[4], and Baojiu Chen(陈宝玖)[5]

[1] *Key Laboratory of Photo-electronic Materials, Ningbo University, Ningbo* 315211, *China*
[2] *Taizhou Special Equipment Inspection and Research Institute, Taizhou* 318000, *China*
[3] *Fujian Provincial Key Laboratory of Functional Marine Sensing Materials, Center for Advanced Marine Sensing Materials and Smart Sensors, Minjiang University, Fuzhou* 350108, *China*
[4] *State Key Laboratory on Integrated Optoelectronics, College of Electronic Science and Engineering and College of Physics, Jilin University, Changchun* 130012, *China*
[5] *Department of Physics, Dalian Maritime University, Dalian* 116026, *China*

(Received 9 January 2022; revised manuscript received 15 March 2022; accepted manuscript online 28 March 2022)

By using an improved Bridgman method, 0.3 mol% Tm^{3+}/0.6 mol% Tb^{3+}/y mol% Eu^{3+} ($y = 0$, 0.4, 0.6, 0.8) doped $Na_5Y_9F_{32}$ single crystals were prepared. The x-ray diffraction, excitation spectra, emission spectra and fluorescence decay curves were used to explore the crystal structure and optical performance of the obtained samples. When excited by 362 nm light, the cool white emission was realized by $Na_5Y_9F_{32}$ single crystal triply-doped with 0.3 mol% Tm^{3+}/0.6 mol% Tb^{3+}/0.8 mol% Eu^{3+}, in which the Commission Internationale de l'Eclairage (CIE) chromaticity coordinate was (0.2995, 0.3298) and the correlated color temperature (CCT) was 6586 K. The integrated normalized emission intensity of the tri-doped single crystal at 448 K could keep 62% of that at 298 K. The internal quantum yield (QY) was calculated to be $\sim$ 15.16% by integrating spheres. These results suggested that the single crystals tri-doped with Tm^{3+}, Tb^{3+} and Eu^{3+} ions have a promising potential application for white light-emitting diodes (w-LEDs).

Keywords: $Tm^{3+}/Tb^{3+}/Eu^{3+}$ triply-doped $Na_5Y_9F_{32}$, white light emission, energy transfer process, thermal stability

PACS: 78.60.Lc, 78.66.Sq **DOI:** 10.1088/1674-1056/ac6160

1. Introduction

Over the years, with the continuous consumption of energy, the growth of energy-efficient equipment has become an unstoppable trend. The white light-emitting diodes (w-LEDs) have aroused high interest due to their advantages of energy-saving, fast switching, longer lifetime, environmentally friendly, compact size, and color tunability over fluorescent tubes and incandescent bulbs.[1–4] Currently, the w-LEDs are mainly obtained in the following ways: (i) the combination of blue chip of GaN/InGaN and yellow phosphor of YAG: Ce^{3+};[5] (ii) mixing three colors (blue, red, green) phosphor to achieve white emission under UV excitation;[6] and (iii) the composition of a unitary NUV/UV LED chip with multicolor fluorescence.[7] The white light produced by the above methods often encounters some problems, such as low efficacy, reduced lifetime, weak resistance to heat and small rendering index, which reduce the quality of the white light.[8–10] Therefore, increasing academic interest has concentrated on the research of pursuing a mono-phase and full-emission material by a near ultraviolet stimulation to overcome the defects of traditional w-LEDs.[11] The unique electron transitions (4f–4f or 4f–5d) in RE^{3+} ions can generate in the aggregate spectral cover scope from ultraviolet to infrared.

Among RE^{3+} ions, Tm^{3+} has a high emission peak ($^1D_2 \rightarrow {}^3F_4$) at $\sim$ 450 nm (blue), and Tb^{3+} usually plays a green-emitting sensitizer at $\sim$ 545 nm (green $^5D_4 \rightarrow {}^7F_5$). Eu^{3+} acts as an effective red-emitting activator owing to the transition of $^5D_0 \rightarrow {}^7F_J$ ($J = 1$, 2, 3, 4).[12] The $Tm^{3+}/Tb^{3+}/Eu^{3+}$ tri-doping used in some materials has been extensively researched, such as $Na_5La(MoO_4)_4$ fluorescent powder: $Tm^{3+}/Tb^{3+}/Eu^{3+}$,[13] and ZnB glasses: $Tm^{3+}/Tb^{3+}/Eu^{3+}$.[14] Nevertheless, owing to the difficulty of crystal growth, the single crystal tri-doped with $Tm^{3+}/Tb^{3+}/Eu^{3+}$ is rarely seen. On account of the $Na_5Y_9F_{32}$ single crystal being proof of invariable physical–chemical properties, thermal stabilization and high luminous efficiency,[15] the RE^{3+} doped $Na_5Y_9F_{32}$ single crystals may be a desirable material to obtain comprehensive performance.

In this paper, the $Tm^{3+}/Tb^{3+}/Eu^{3+}$ doped $Na_5Y_9F_{32}$ single crystals were grown by the Bridgman method. When the excitation wavelength was set at 362 nm, the $Tm^{3+}/Tb^{3+}/Eu^{3+}$ tri-doped $Na_5Y_9F_{32}$ single crystals had abundant emission from 430 nm to 650 nm and the cool white emission was obtained with CIE coordinate (0.2995, 0.3298)

†Corresponding author. E-mail: hpxcm@nbu.edu.cn
‡Corresponding author. E-mail: wjnaf@163.com

© 2022 Chinese Physical Society and IOP Publishing Ltd

and the CCT of 6586 K.

2. Experimental details

By using through the ameliorative Bridgman technique, Tm^{3+}, $Tb^{3+}$and Eu^{3+} doped $Na_5Y_9F_{32}$ single crystals were prepared from 99.99% high purified NaF, YF_3, TmF_3, TbF_3 and EuF_3 powders. Moreover, adding a slight of KF (99.99%) as flux into raw material to change the phase equilibrium between YF_3 and NaF and reduce the crystalline temperature of $Na_5Y_9F_{32}$ single crystal.[16] The homologous concrete course of crystal growth was described elsewhere.[17] Here, the $Na_5Y_9F_{32}$ single crystal is named as NYF, and the RE^{3+} singly doped, co-doped and tri-doped are as below:

Sample A: NYF + 0.3 TmF_3;
Sample B: NYF + 0.6 TbF_3;
Sample C: NYF + 0.6 EuF_3;
Sample D: NYF + 0.6 TbF_3 + 0.3 TmF_3;
Sample E: NYF + 0.6 TbF_3 + 0.3 TmF_3 + 0.4 EuF_3;
Sample F: NYF + 0.6 TbF_3 + 0.3 TmF_3 + 0.6 EuF_3;
Sample G: NYF + 0.6 TbF_3 + 0.3 TmF_3 + 0.8 EuF_3.

As displayed in Fig. 1(e), the size of the grown lucent crystal is approximately Φ10 mm×30 mm. It was then cut and burnished to ∼ 2 mm to test correlative luminescence properties. As listed in Table 1, the real Tm^{3+}, Tb^{3+} and Eu^{3+} contents in $Na_5Y_9F_{32}$ single crystal were determined by ICP-AES from PerkinElmer Inc Optima 3000. The crystalline phase of the as obtained samples was verified via Bruker D8 Advance (Germany) with radiation source of Cu-K-α ray (0.15043 nm). The excitation spectra, emission spectra, and decay lifetime were investigated by FLSP 920 type spectrometer (Edinburgh, England). The FLSP 920 spectrometer with temperature controlling equipment was used to explore temperature-dependent emission spectra. The quantum yield was measured by Horiba FL3-111 spectrometer (France).

Table 1. The doping concentrations of Tm^{3+}, Tb^{3+}, Eu^{3+} in raw material and the ionic numbers of Tm^{3+}, Tb^{3+} and Eu^{3+} ions in the obtained crystal.

Sample	A	B	C	D	E	F	G
Tm^{3+} (mol% in raw material)	0.3	0	0	0.3	0.3	0.3	0.3
Measured Tm^{3+} (mol% in single crystal)	0.302	0	0	0.304	0.307	0.303	0.305
Tb^{3+} (mol% in raw material)	0	0.6	0	0.6	0.6	0.6	0.6
Measured Tb^{3+} (mol% in single crystal)	0	0.566	0	0.564	0.571	0.575	0.578
Eu^{3+} (mol% in raw material)	0	0	0.6	0	0.4	0.6	0.8
Measured Eu^{3+} (mol% in single crystal)	0	0	0.475	0	0.306	0.486	0.648

3. Results and discussion

3.1. XRD analyses

Figures 1(a)–1(d) exhibit the XRD patterns of $Na_5Y_9F_{32}$ (PDF#27-1428), samples A, D and G, respectively. The whole diffraction peaks are tallied with standard data and there are no unnecessary peaks. It suggests that introduced Tm^{3+}, Tb^{3+} and Eu^{3+} ions will not have major influence on the crystal structure of $Na_5Y_9F_{32}$. Davolos recommends that in order to implement effective ions doping, the permissible radius differences between the dopants and substitution sites should be not greater than 30%.[18] The percentage differences in radius of Tm^{3+}–Y^{3+}, Tb^{3+}–Y^{3+} and Eu^{3+}–Y^{3+} are 2.58%, 3.36% and 6.38%, respectively, demonstrating that the three ions are efficiently doped into $Na_5Y_9F_{32}$ single crystal.

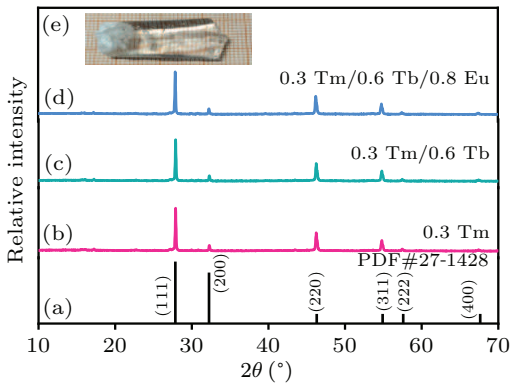


Fig. 1. (a) The XRD patterns of the standard XRD cards of $Na_5Y_9F_{32}$ (PDF#27-1248). (b)–(d) XRD patterns for 0.3 mol% Tm^{3+}, 0.3 mol% Tm^{3+}/0.6 mol% Tb^{3+} and 0.3 mol% Tm^{3+}/0.6 mol% Tb^{3+}/0.8 mol% Eu^{3+} doped single crystals using the powders obtained by grinding the bulk crystal. (e) The insert diagram is a picture of grown $Na_5Y_9F_{32}$ single crystal.

3.2. Excitation spectra and emission spectra

Figure 2 demonstrates the emission and excitation spectra of Tm^{3+}, Tb^{3+} and Eu^{3+} singly doped single crystals. Figures 2(a)–2(c) present the excitation spectra of Tm^{3+}, Tb^{3+} and Eu^{3+} singly doped ones monitored at 452 nm, 544 nm and 614 nm, respectively. Figure 2(a) reveals a sharp peak at 358 nm, owing to $^3H_6 \rightarrow {}^1D_2$ transition of Tm^{3+}. Figure 2(b) illustrates five peaks at 320 nm, 338 nm, 354 nm, 370 nm and 378 nm, which originate from the ground sate $^7F_6$ to excitation sates $^5D_1$, $^7F_6$, $^5L_8$, $^5D_2$, $^5G_6$ and $^5D_3$ transitions of Tb^{3+}. Figure 2(c) consists of 362 nm, 383 nm and 396 nm three peaks, originating from $^7F_0 \rightarrow {}^5D_4$, $^5G_2$ and $^5L_6$ transitions of Eu^{3+}. It is noted that the Tm^{3+}, Tb^{3+} and Eu^{3+} excitation spectra show a consistent excitation band at about 362 nm, indicating the three ions may be stimulated by 362 nm simultaneously, which offer a potential possibility for white emission through the integration of a near-ultraviolet LED chip with Tm^{3+}/Tb^{3+}/Eu^{3+} triply-doped $Na_5Y_9F_{32}$ single crystal. Figures 2(d)–2(f) show the emission spectra of Tm^{3+}, Tb^{3+} and Eu^{3+} doped ones, respectively, stimulated by 362 nm. Fig-

ure 2(d) exhibits a blue band located at 452 nm, which is due to the transition of Tm^{3+} : $^1D_2 \rightarrow {}^3F_4$. Figure 2(e) describes the peaks at 486 nm, 544 nm, which are owing to $^5D_4 \rightarrow {}^7F_6$, $^7F_5$ transitions of Tb^{3+}, respectively. Because of the $^5D_0 \rightarrow {}^7F_1$, $^7F_2$ transitions of Eu^{3+}, two emission bands are presented at 592 nm and 613 nm in Fig. 2(f). Generally speaking, the ligand field makes no difference to the $^5D_0 \rightarrow {}^7F_1$ transition intensity of the magnetic dipolar, while the $^5D_0 \rightarrow {}^7F_2$ transition of electric dipolar is known to be prohibited in central symmetric environment.[19] The emission intensity of the transition $^5D_0 \rightarrow {}^7F_1$ (592 nm) is stronger than that of $^5D_0 \rightarrow {}^7F_2$ (613 nm) in Fig. 3(f), which manifests that the local structure of Eu^{3+} in $Na_5Y_9F_{32}$ single crystal belongs to spatial inversion.

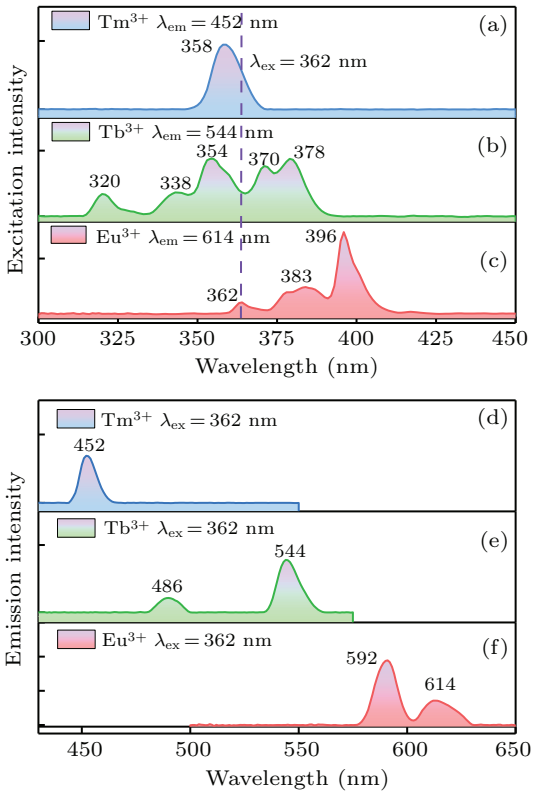


Fig. 2. (a)–(c) Excitation spectra of sample A: Tm^{3+}, B: Tb^{3+} and C: Eu^{3+}, respectively. (d)–(f) Emission spectra of sample A: Tm^{3+}, B: Tb^{3+} and C: Eu^{3+}, respectively.

Figure 3(a) exhibits the fluorescence spectra of 0.3 mol% Tm^{3+}/0.6 mol% Tb^{3+}/y mol% Eu^{3+} ($y = 0.4$, 0.6, 0.8) tri-doped $Na_5Y_9F_{32}$ crystals. Under 362 nm excitation, the fluorescence spectra show the blue, green and reddish-orange emission, which originate from Tm^{3+} : $^1D_2 \rightarrow {}^4F_3$ (452 nm), Tb^{3+} : $^5D_4 \rightarrow {}^7F_6$ (491 nm), Tb^{3+} : $^5D_4 \rightarrow {}^7F_5$ (544 nm), and Eu^{3+} : $^5D_0 \rightarrow {}^7F_1$ (591 nm), Eu^{3+} : $^5D_0 \rightarrow {}^7F_2$ (613 nm), respectively. Figure 3(b) shows the emission intensity of Tm^{3+}, Tb^{3+} and Eu^{3+} with relation to the Eu^{3+} content. With the addition of Eu^{3+} concentration, the luminescence intensities of Tm^{3+} and Tb^{3+} decrease, while the luminescence intensity of Eu^{3+} increases gradually.

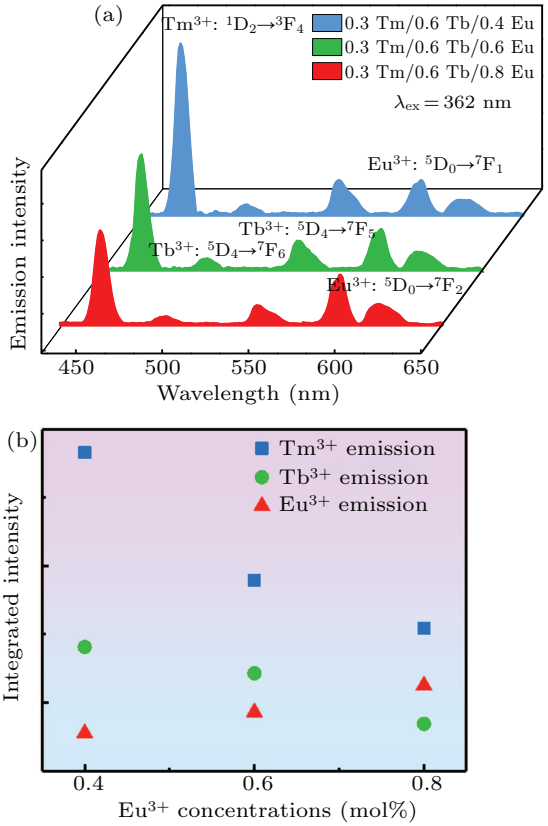


Fig. 3. (a) Fluorescence spectra of samples E, F and G in the wavelength of 430 nm–650 nm under 362 nm excitation. (b) The relationship between integrated emission intensity with different Eu^{3+} concentration.

3.3. Energy transfer

The possible energy transfer among Tb^{3+}, Tm^{3+} and Eu^{3+} ions have been investigated previously.[20,21] Here, an explicit level scheme was made to make clear the procedure of energy transfer in Fig. 4. Under excitation upon of 362 nm, the Tm^{3+} ions in ground-state are stimulated to $^1D_2$ energy level by absorbing the pumping energy, then the ions in high energy level release a part of the energy to $^1G_4$ level through non-radiative transition (NR). Simultaneously, the energy of $^1G_4$ attenuates to the $^6H_3$ level with 452 nm (blue) radiation. The Tb^{3+} ions in the ground state absorb the excitation energy and then jump to the $^5D_2$ energy level. Because the particles do not have a stable state at $^5D_2$ energy level, so they will nonradiative relax to the $^5D_4$ energy level. Meanwhile, 491 nm and 544 nm (green) radiations are produced, which originate from the transitions: $^5D_4 \rightarrow {}^7F_6$, $^5D_4 \rightarrow {}^7F_5$ of Tb^{3+}, respectively. Similarly, the Eu^{3+} ions in the ground state are excited into the $^5D_4$, then the transitions of Eu^{3+} : $^5D_0 \rightarrow {}^7F_1$ (591 nm), Eu^{3+} : $^5D_0 \rightarrow {}^7F_2$ (613 nm) will occur.

It can be known from the absorption spectra in Fig. 4, the energy levels between $^1G_4$ and $^2D_5$ (5×10^3 cm^{-1}), $^5D_4$ and $^5D_1$ (2×10^3 cm^{-1}) are very small. It is expected that the processes of the energy transfer (ET) is easily to occur. Significantly, the ET1 and ET2 will easily occur when Tb^{3+}, Tm^{3+} and Eu^{3+} ions are in a system. It can be observed that

the transitions of $Tm^{3+}:{}^1G_4 \rightarrow Eu^{3+}:{}^2D_5$ (592 nm) and $Tb^{3+}:{}^5D_4 \rightarrow Eu^{3+}:{}^5D_1$ (614 nm) are generated under the influence of both ET1 and ET2 processes. These two processes will expedite the non-radiative transition of $Tm^{3+}:{}^1D_2 \rightarrow {}^1G_4$ and $Tb^{3+}:{}^5D_2 \rightarrow {}^5D_4$ due to the depression in $Tm^{3+}:{}^1G_4$ and $Tb^{3+}:{}^5D_4$. Thus, the Tb^{3+} and Tm^{3+} emission intensities drop sharply, while the luminous intensity of Eu^{3+} ascends, which is identical to the changes of Fig. 3(b).

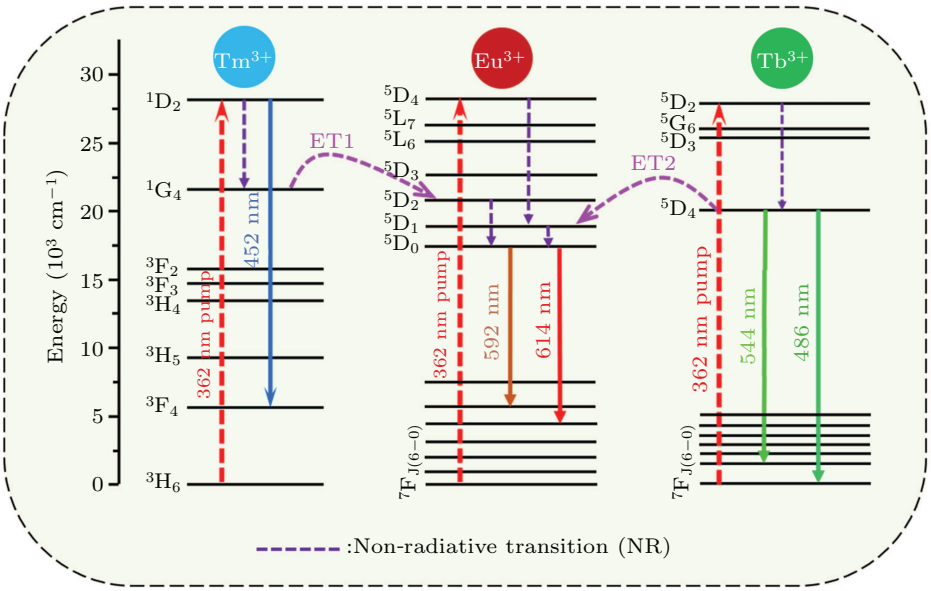


Fig. 4. Schematic illustration of the energy transfers in $Tm^{3+}/Tb^{3+}/Eu^{3+}$ tri-doped $Na_5Y_9F_{32}$ single crystal.

3.4. Decay curves and CIE

To further describe the energy transfer processes among Tm^{3+}, Tb^{3+} and Eu^{3+} ions, Fig. 5 reveals the decay curves of Tb^{3+}: 542 nm and Tm^{3+}: 452 nm when pumped at 362 nm. The measured data is excellently assessed by the double exponential fitting[22,23]

$$\tau = (A_1\tau_1^2 + A_2\tau_2^2)/(A_1\tau_1 + A_2\tau_2), \tag{1}$$

where τ_1 and τ_2 are the rapid and slow lifetimes for exponential components, respectively. A_1 and A_2 are the correlative parameters obtained by fitting.

According to the average time obtained by calculation, the efficiency of ET1 and ET2 can be ascertained by the formula[24,25]

$$\eta_{ET} = 1 - \frac{\tau_s}{\tau_0}, \tag{2}$$

where τ_0 is the average time of sample D at 452 nm and 544 nm in the absence of Eu^{3+}, and τ_s is the average time of samples E, F, G at 452 nm and 544 nm in the presence of Eu^{3+}. Table 2 lists the detailed lifetimes and the energy transfer efficiencies. In Table 2, as the Eu^{3+} concentration increases, the lifetimes of Tm^{3+}: 452 nm, Tb^{3+}: 544 nm decrease, while the energy transfer efficiency increases gradually, indicating the possible energy transfer of $Tm^{3+} \rightarrow Eu^{3+}$, $Tb^{3+} \rightarrow Eu^{3+}$.

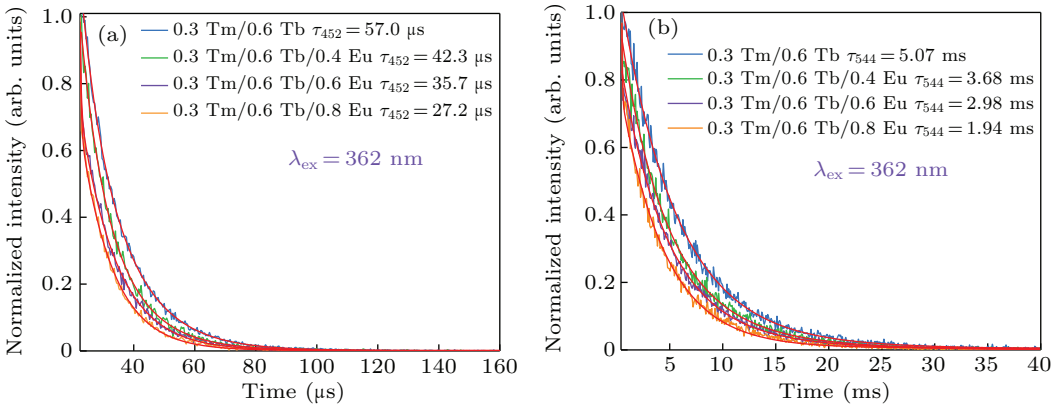


Fig. 5. (a) Decay curves of the samples D, E, F and G at 452 nm. (b) The samples D, E, F and G at 544 nm, respectively. The red line is a nonlinear fitting.

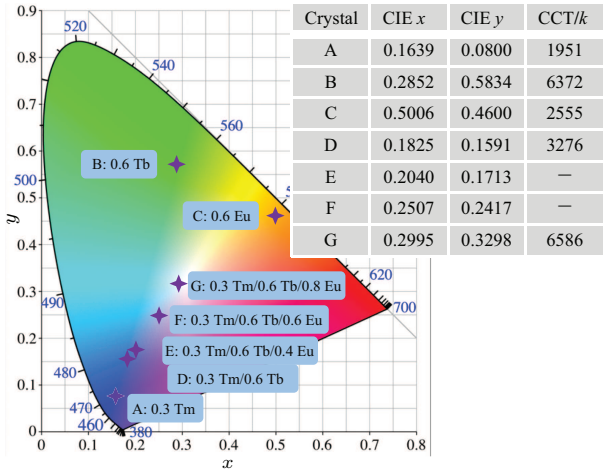
Table 2. The average decay lifetimes of the 452 nm, 544 nm and energy transfer efficiencies of ET1, ET2 when excited by 362 nm.

Samples	τ_{452} (μs)	τ_{544} (ms)	ETE1	ETE2
D	57.0	5.07	/	/
E	42.3	3.68	25.8%	27.4%
F	35.7	2.98	37.4%	41.2%
G	27.2	1.94	52.3%	61.7%

Figure 6 presents the CIE chromaticity coordinates and CCT of the prepared crystals. In Fig. 6, the color of the emitted light changes from blue to cool white, emission accompanied by increasing the Eu^{3+} content. Furthermore, the CCT can be defined by[26]

$$\mathrm{CCT} = -437n^3 + 3601n^2 - 6861n + 5514.31, \tag{3}$$

where $n = (x - 0.3320)/(y - 0.1858)$, x and y are CIE chromaticity coordinates. When the Eu^{3+} concentration comes to 0.8 mol%, the CIE chromaticity coordinates and CCT are (0.2995, 0.3298) and 6586 K, which suggest that cool white emission can be realized in $Na_5Y_9F_{32}$ single crystal when pumped at 362 nm.



Crystal	CIE x	CIE y	CCT/k
A	0.1639	0.0800	1951
B	0.2852	0.5834	6372
C	0.5006	0.4600	2555
D	0.1825	0.1591	3276
E	0.2040	0.1713	–
F	0.2507	0.2417	–
G	0.2995	0.3298	6586

Fig. 6. The chromaticity CIE diagram of prepared samples under 362 nm excitation. The inset table shows the detailed values of color coordinates and correlated temperatures.

3.5. Quantum yield and temperature-dependent emission spectra

The quantum yield is a factor that can not be ignored, as is depicted in Fig. 7. The QY of prepared sample G is measured by the integrating sphere and can be confirmed by the equation[27,28]

$$\mathrm{QY} = \frac{E_\mathrm{B} - E_\mathrm{A}}{S_\mathrm{A} - S_\mathrm{B}}, \tag{4}$$

where E_A and E_B are the integrated emission intensities of the $BaSO_4$ powder reference and the sample, respectively. S_A and S_B are the integrated scattered intensities of the reference $BaSO_4$ powder and the sample, respectively. The QY equals to ∼ 15.16%. According to the previous reports, we found that the value of 1 mol% Dy^{3+}/0.8 mol% Sm^{3+} co-doped $Na_5Y_9F_{32}$ single crystal is higher than that of Tb^{3+}/Eu^{3+} co-doped GC containing KY_3F_{10} (13%),[29] Dy^{3+}/Eu^{3+} co-doped $LiLuF_4$ single crystal (11%),[30] and Ce^{3+}/Tb^{3+} co-doped $Li_3Sc_2(PO_4)_3$ (9%).[31] The present $Tm^{3+}/Tb^{3+}/Eu^{3+}$ co-doped $Na_5Y_9F_{32}$ single crystal shows relatively high internal quantum efficiency.

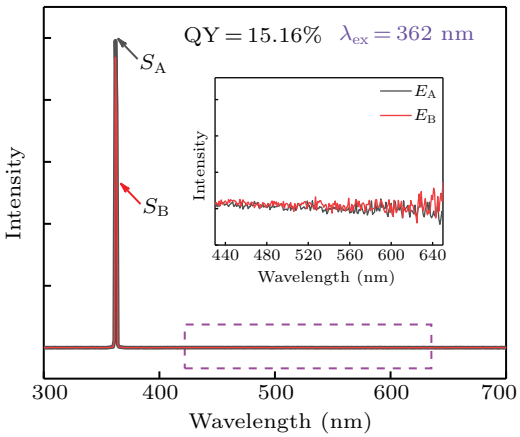


Fig. 7. The absorption and emission spectra collected by an integrating sphere to calculate the quantum yield of sample G. The inset is the enlarged part, which is marked with a dashed blue line.

When white light sources are developed and applied in real life, many other parameters need to be considered. Thermal stability is also a crucial parameter, which can heavily affect the function of white LED devices.[32] Generally speaking, the optical materials are subjected to a thermal quenching, which means that the emission intensity will continue to weaken when elevating the working temperature. Hence, it is essential to study the temperature-dependent behaviors of the obtained crystals.

Figure 8(a) displays the temperature-dependent emission spectra of the sample G within the range of 300 K–450 K. It is clearly observed that the emission intensity decreases with the rise of the temperature. As described in Fig. 8(b), the normalized emission intensity of the sample G at 450 K retains about 64% of the initial intensity at 300 K. The value is superior to that of the Y_2SiO_5 phosphor: $Ce^{3+}/Tb^{3+}/Eu^{3+}$ (∼ 21%);[33] the oxide glasses: Bi^{3+}/Eu^{3+} (∼ 46%).[34] Indicating that the $Na_5Y_9F_{32}$ crystal has excellent stability as a matrix carrier. This probably relates to phonon interaction in the host matrix. The result implies that the $Na_5Y_9F_{32}$ single crystal possesses good thermal stability within the range of 300 K–450 K. Simultaneously, the activation energy (ΔE) is also calculated by the following formula:[35,36]

$$I_T = I_0\left[(1 + A\exp(\Delta E/KT)\right]^{-1}, \tag{5}$$

where I_0 is the initial intensity at 300 K, I_T represents the intensity at temperature T, A presents a constant and K is 8.617×10^{-5} eV. ΔE is equivalent to 0.271 eV from the fitting slope in Fig. 9(b). The value is higher than that of $K_3La(PO_4)_2$ phosphors: $Tm^{3+}/Tb^{3+}/Eu^{3+}$ (0.2 eV).[37] All evidence hints that the $Na_5Y_9F_{32}$ single crystal triply doped with $Tm^{3+}/Tb^{3+}/Eu^{3+}$ possesses good thermal stability.

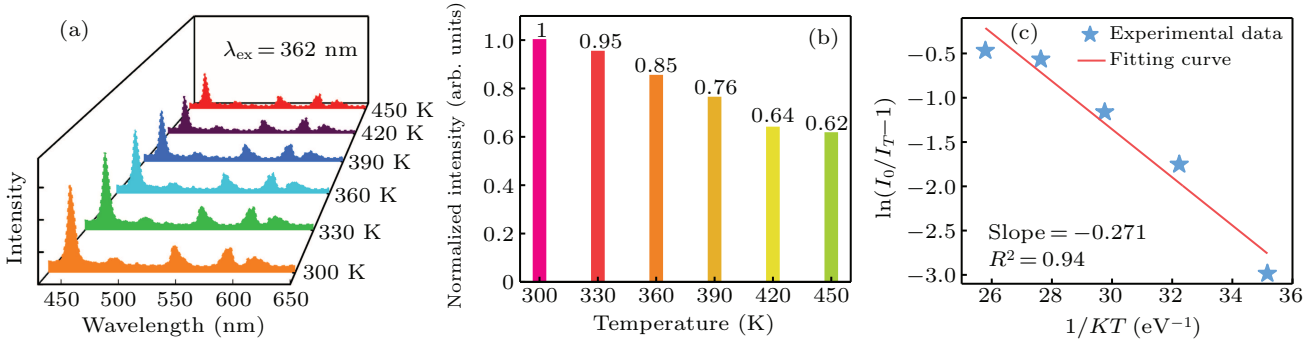


Fig. 8. (a) Temperature-dependent emission spectra of the sample G under 362 nm light excitation. (b) Normalized integrated emission intensity in a temperature range from 300 K to 450 K. (c) The plot of $\ln(I_0/I_T - 1)$ against $1/(KT)$ for crystal G.

4. Conclusion

Our experiment demonstrated that Tm^{3+}, Tb^{3+} and Eu^{3+} ions could be effectively incorporated together into $Na_5Y_9F_{32}$ single crystals. The color of the obtained samples was shifted from blue to white by adjusting the content of Eu^{3+} under 362 nm excitation. The existence of the energy transfers of $Tm^{3+} \rightarrow Eu^{3+}$ (ET1) and $Tb^{3+} \rightarrow Eu^{3+}$ (ET2) was fully proved by their emission spectra, fluorescence lifetimes and the energy transfer efficiencies of ET1 and ET2 were estimated as 52.3% and 61.7%, respectively. Importantly, an ideal cool white emission was obtained from sample G with CIE coordinate (0.2995, 0.3298).

Moreover, the emission intensity of the obtained sample could still maintain $\sim 62\%$ high at 450 K with an activation energy (0.271 eV). The QY of the sample was counted as $\sim 15.16\%$. All these findings hint that $Na_5Y_9F_{32}$ crystal triply doped with Tm^{3+}, Tb^{3+} and Eu^{3+} has a good future in w-LED applications.

Acknowledgements

Project supported by the National Natural Science Foundation of China (Grant No. 62275133), the Natural Science Foundation of Zhejiang Province of China (Grant No. LY22E020002), the Natural Science Foundation of Ningbo (Grant Nos. 2021J077 and 202003N4099), and K.C. Wong Magna Fund in Ningbo University.

References

[1] Xiao F, Yi R, Yuan H, Zang G and Xie C 2018 *Spectrochim. Acta A* **202** 352
[2] Ray S, Tadge P, Dutta S, *et al.* 2018 *Ceramics International* **44** 8334
[3] Jha K, Vishwakarma A K, Jayasimhadri M and Haranath D 2017 *J. Alloys Compd.* **719** 116
[4] Chang J, Chen C, Rudysh M, Brik M G, Piasecki M and Liu W 2019 *J. Lumin.* **206** 417
[5] Chen D, Zhou Y and Zhong J A 2016 *RSC Advances* **6** 86285
[6] Wang X, Li X, Xu S, *et al.* 2020 *J. Asian Ceram. Soc.* **8** 1066
[7] Kang F W, Hu Y H, Wu H Y, *et al.* 2011 *Chin. Phys. Lett.* **28** 107201
[8] Dai P and Ma R 2020 *J. Alloys Compd.* **812** 152143
[9] Mungra M, Steudel F, Ahrens B, *et al.* 2017 *Journal of Luminescence* **192** 71
[10] Yu M, Xu X, Zhang W, Chen X, Zhang P and Huang Y 2020 *J. Alloys Compd.* **817** 152761
[11] Shang M, Li C and Lin J 2014 *Chem. Soc. Rev.* 43 1372
[12] Liu Y, Liu G, Wang J, *et al.* 2014 *Inorg. Chem.* **53** 11457
[13] Jin Y, Lu W, Zhang J, *et al.* 2014 *J. Nanosci Nanotechno.* **14** 3683
[14] Naresh V, Gupta K, Reddy C P and Ham B S 2017 *Spectrochim. Acta A* **175** 43
[15] Qiao Y, Zhou X, Zhang J, *et al.* 2020 *J. Alloys Compd.* **824** 153987
[16] Qiao Y, Zhou X, Zhang J, Xia H, Song H and Chen B 2020 *Infrared Phys. Techn.* **105** 103183
[17] Wang H, Xia H, Hu J, Zhu Y and Chen B 2018 *J. Alloys Compd.* **765** 1035
[18] LeJemtel T H, Keung E, Sonnenblick E H, *et al.* 1979 *Circulation* **59** 1098
[19] Chen D, Yu Y, Huang P, *et al.* 2010 *Acta Mater.* **58** 3035
[20] Liu X, Chen G, Chen Y and Yang T 2017 *J. Non-Cryst Solids* **476** 100
[21] Xu M, Ding Y, Luo W, *et al.* 2020 *Optics & Laser Technology* **121** 105829
[22] Li B, Wang S, Sun Q, Lu C, Guo H and Huang X 2018 *Dyes Pigments* **154** 252
[23] Cao J, Wang X, Li X, Wei Y, Chen L and Guo H 2016 *J. Lumin.* **170** 207
[24] Jiao M, Guo N, Lü W, *et al.* 2013 *Inorganic Chem.* **52** 10340
[25] Chen C, Gu Z, Li Q and Zhang Y 2020 *J. Eur. Ceram. Soc.* **40** 4595
[26] Du P and Yu J S 2015 *J. Alloys Compd.* **653** 468
[27] Luo D, Chen Q, Liu B, *et al.* 2019 *Polymers* **11** 384
[28] Beck A R, Das S and Manam J 2017 *J. Mater. Sci.* **28** 17168
[29] Xu F, Fang L, Zhou X, *et al.* 2020 *Opt. Mater.* **108** 110222
[30] Yu B, Zheng B, Xia H, *et al.* 2021 *Ceram. Int.* **47** 9668
[31] Jiao M, Xu Q, Liu M, *et al.* 2018 *Chem. Phys.* **20** 26995
[32] Li Q, Zhang S, Lin W, Li W, Li Y, Mu Z and Wu F 2020 *Spectrochim. Acta A* **228** 117755
[33] Zhang X, Zhou L, Pang Q, *et al.* 2014 *J. Phys. Chem. C* **118** 7591
[34] Giraldo O G, Fei M, Wei R, Teng L, Zheng Z and Guo H 2020 *J. Lumin.* **219** 116918
[35] Li J Y, Hou D, Zhang Y, Li H, Lin H, Lin Z, Zhou W and Huang R 2019 *J. Lumin.* **213** 184
[36] Som S, Das S, Dutta S, et al. 2015 *RSC Advances* **5** 70887
[37] Jiao Y, Wu X, Ren Q, *et al.* 2019 *Optics & Laser Technology* **109** 470